

Structural, dielectric properties and electrical conduction behaviour of Dy substituted $\text{CaCu}_3\text{Ti}_4\text{O}_{12}$ ceramics

Raman Kashyap^a, R.K. Mishra^a, O.P. Thakur^b, R.P. Tandon^{a,*}

^aDepartment of Physics and Astrophysics, University of Delhi, Delhi 110007, India

^bSolid State Physics Laboratory, Timarpur, Delhi 110054, India

Received 19 April 2012; received in revised form 23 May 2012; accepted 23 May 2012

Available online 8 June 2012

Abstract

Dy substituted CCTO ceramics were synthesized using solid state reaction method. Effect of Dy on structural, microstructural, dielectric and electrical properties has been studied over a wide temperature (300–500 K) and frequency range (100 Hz–1 MHz). Rietveld refinement, carried out on the samples, confirmed single phase formation and indicated overall decrease in lattice constant. Microstructure showed bimodal distribution of grains in CCTO with bigger grains surrounded by smaller grains. Dy substitution reduced grain size. Dy substitution in CCTO reduces the dielectric constant which may be attributed to increase of the Schottky potential barrier. The dielectric constant remains nearly constant in temperature range 300–400 K. The AC conductivity obeys a power law, $\sigma_{ac} = A f^n$, where n is the temperature dependent frequency exponent. The AC conductivity behaviour can be divided into three regions, over entire temperature range, depending on conduction processes. The relevant charge transport mechanisms have been discussed.

© 2012 Elsevier Ltd and Techna Group S.r.l. All rights reserved.

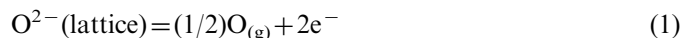
Keywords: A. Powders: solid state reaction method; B. Grain boundaries; C. Dielectric properties; C. Electrical conductivity

1. Introduction

In the electronic devices based on capacitive components, it is the dielectric constant which determines the degree of miniaturization of device. Calcium Copper Titanate (CCTO) with the chemical formula $\text{CaCu}_3\text{Ti}_4\text{O}_{12}$ is attracting attention due to its colossal dielectric constant. Dielectric constant exhibited by CCTO ceramics remains almost constant over a wide range of temperature (100–600 K) [1]. CCTO is a bcc structured material with the space group $\text{Im}\bar{3}$ [2] and shows no change in crystal structure down to 35 K [1]. Various explanations have been given to understand the origin of colossal dielectric constant in CCTO ceramics [1–5]. Internal Barrier Layer Capacitance (IBLC) mechanism is widely accepted for explaining the origin of high value of dielectric constant shown by CCTO ceramics [3,4,6]. IBLC mechanism states

that conducting grains and insulating grain boundaries give rise to high value of dielectric constant. It has been observed that dielectric and microstructural properties in CCTO are processing conditions dependent. Size of grain and thickness of grain boundaries generally depend on sintering duration [7].

The origin of semiconductivity in CCTO ceramics has been explained in two ways, first in terms of oxygen vacancies generated according to following equation:



where electrons enter the Ti 3d conduction band and this can be represented by Ti^{3+} in the formula $\text{CaCu}_3\text{Ti}_{4-x}\text{Ti}^{3+}\text{O}_{12-x/2}$ [6] and, secondly [8] where it is suggested that Cu^{2+} reduces to Cu^+ slightly and in order to maintain the oxidation state, a slight substitution of Ti^{4+} on Cu site compensates. During cooling, Cu^+ oxidises to Cu^{2+} , releasing electrons into the Ti 3d conduction band as $\text{Ca}^{2+}(\text{Cu}_{1-x}\text{Ti}_x^{4+})_3(\text{Ti}_{4-6x}\text{Ti}_6^{3+})\text{O}_{12}$, where a very small amount of 'x' would affect conductivity without being detected in the x-ray diffraction data. CCTO ceramics are

*Corresponding author. Tel.: +91 11 27667725 1367;

fax: +91 11 27667061.

E-mail address: ram_tandon@hotmail.com (R.P. Tandon).

reported to exhibit the ferroelectric-like hysteresis loop [9,10] which is quite enigmatic as these ceramics have been assumed as non-ferroelectric owing to their bcc structure and Im3 space group [2]. CCTO shows the ferroelectric-like relaxor behaviour. Relaxor ferroelectrics are a class of compositionally disordered, structurally-frustrated incipient ferroelectrics [11].

Electrical measurements are most sensitive and versatile tool for the investigation of conduction mechanisms in solids. In the present paper, we investigate the role of Dy substitution on the structural, dielectric properties and electrical conduction behaviour of CCTO ceramics over a wide temperature and frequency range.

2. Experimental details

Pure CCTO and Dy doped samples were prepared using the solid state reaction method. Precursors, CuO (99%, Thomas Baker), TiO₂ (99%, Loba Chemie), CaCO₃ (99.5%, Sisco Research Laboratories Pte. Ltd.) and Dy₂O₃ (99.9%, Rare Earth Pte Ltd.) were taken in stoichiometric amount according to Ca_{1-3x/2}Dy_xCu₃Ti₄O₁₂ ($x=0, 0.02, 0.04, 0.06, 0.08, 0.10$). Samples with $x=0.0, 0.02, 0.04, 0.06, 0.08$, and 0.10 will be hereafter represented by C0, C2, C4, C6, C8 and C10, respectively. Powders were ball milled for 12 h in the distilled water with zirconia ball as grinding media. Milled powders were dried at 353 K for 24 h in oven. Dried powders were then grounded using mortar–pestle and then calcined at 1173 K for 5 h. Calcined powders were again grounded using mortar–pestle. Room temperature x-ray diffraction (Bruker, D8 Discover) analysis was done on calcined powders. Calcined powders were then pressed into pellets of diameter 13 mm and thickness $\sim 3\text{--}4$ mm using polyvinyl alcohol (PVA) as binder. Green pellets were sintered at 1373 K using heating rate of 3 K/min for 2 hrs and furnace cooled. These pellets were lapped to ~ 1 mm thickness using silicon carbide abrasive powder and then cleaned using ultrasonicator for 15 min in distilled water. Pellets were dried at 363 K for 2 h. Microstructure and elemental analysis of fractured surfaces was recorded using Scanning Electron Microscope (SEM) (Zeiss, MA15) having EDS attachment. Gold was sputtered on both faces of the pellets for making electrical contacts. Impedance analyser (Wayne Kerr 6500B) was used for the dielectric measurement as a function of frequency and temperature.

3. Results and discussion

3.1. x-ray analysis

Fig. 1(a) shows the XRD patterns of pure and Dy doped CCTO samples. XRD analysis confirms the single phase formation with no traces of impurities. Rietveld refinement was carried out for all the samples which further confirmed single phase formation. Fig. 1(b) shows the Rietveld refinement plot for CCTO done by using the software

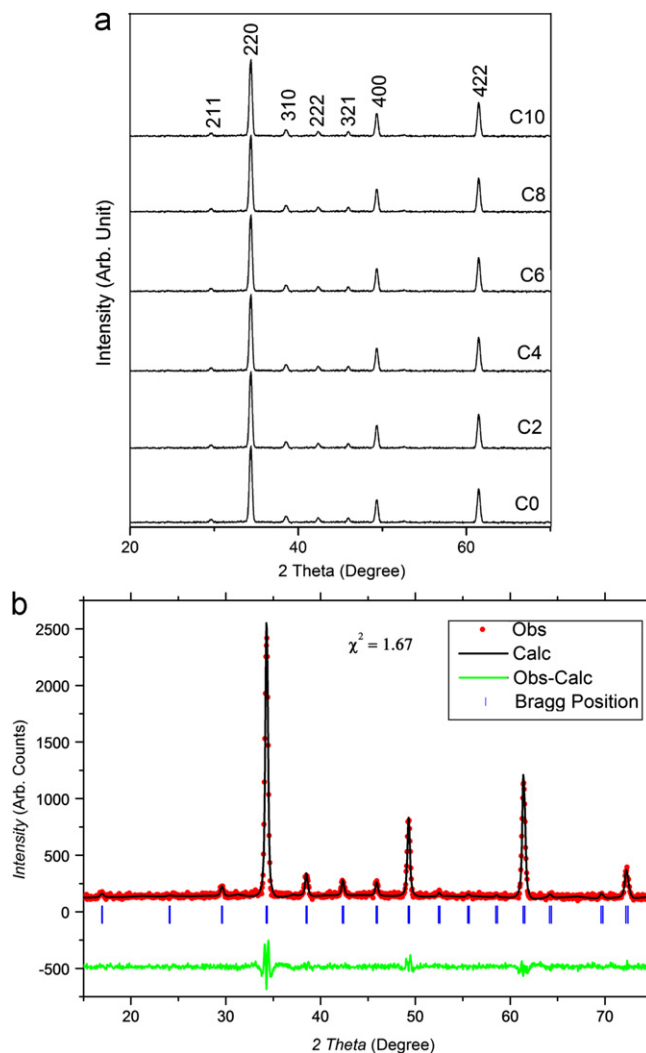


Fig. 1. (a) XRD patterns of pure and Dy doped CCTO samples. (b) Rietveld refined XRD patterns of CCTO ceramic where Obs and Calc represent observed and calculated data, respectively.

FULLPROOF. Refinement for all the samples gave goodness of fit (χ^2) in the range 1–2 indicating the reliability of refined structural parameters. Refined lattice parameters for samples C0, C2, C4, C6, C8 and C10 are found to be 7.3938 Å, 7.3870 Å, 7.3872 Å, 7.3871 Å, 7.3850 Å and 7.3860 Å, respectively.

3.2. Microstructure analysis

SEM images of fractured surface of pure and Dy doped ceramics are shown in Fig. 2(a). SEM image of CCTO shows the bimodal distribution of grains where bigger grains are surrounded by smaller grains. Substitution of Dy in CCTO greatly affects the microstructure. Grain size decreases with the addition of Dy content. Pure CCTO shows larger grains (5–14 μm) surrounded by smaller one (1–5 μm) whereas for subsequent doping concentrations, grain size decreases to the range 0.5–5 μm. It is observed

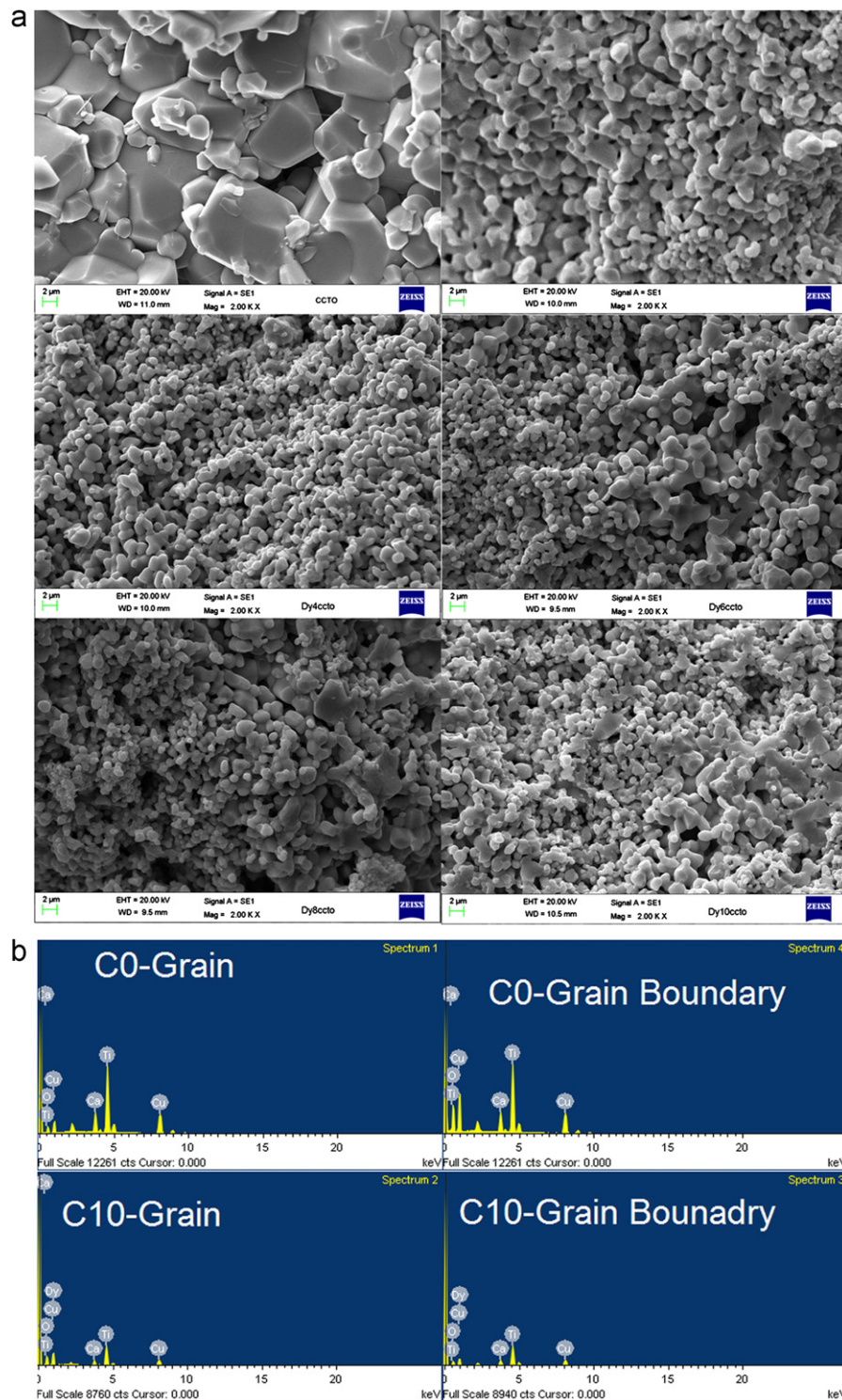


Fig. 2. (a) SEM images of pure and Dy doped samples and (b) EDS spectrum images of samples C0 and C10.

that for higher doping concentrations such as 8 and 10 mol% grains start coalescing.

Energy spectrum (Fig. 2b) of elemental analysis performed on different regions of fractured surface of C0 and C10 doped samples gives insight into the proportion of different elements in different regions. Table 1 gives the wt% of elements found in different regions of Dy doped CCTO samples. It is observed

that with the increase of Dy content, grain and grain boundary also reflect increased concentration of Dy by EDS analysis. Major content of Dy was found in grain than in grain boundary region. Lesser Dy content along the grain boundary may be the major cause for the refinement in grain size. Intermediate Dy contents yielded same qualitative behaviour and hence not included in Fig. 2(b).

Table 1
Elemental proportion in samples C0 and C10 as per EDS.

Sample name	Element	Grain (wt%)	Grain boundary (wt%)
C0	Ca	6.13	6.02
	Ti	30.66	31.28
	Cu	32.19	31.48
	O	31.03	31.22
C10	Ca	5.18	5.26
	Ti	30.40	31.22
	Cu	30.02	30.61
	O	30.51	30.95
	Dy	3.88	1.97

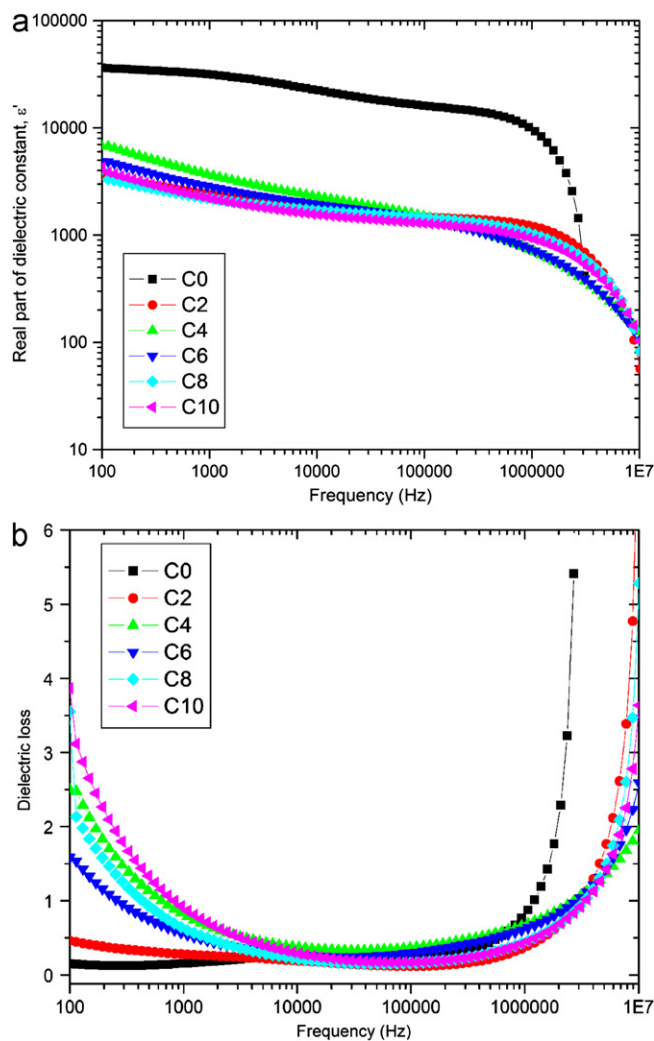


Fig. 3. (a) Variation of real part of dielectric constant ϵ' with frequency for pure and Dy doped samples and (b) frequency dependence of dielectric loss for pure and Dy doped CCTO samples.

3.3. Dielectric properties

Fig. 3(a) shows the frequency variation of real part of dielectric constant (ϵ') of pure and Dy doped CCTO ceramics. Dielectric constant of doped samples C2, C4, C6, C8 and C10 at 10 kHz reduces by an order when compared with pure CCTO at room temperature. Dielectric constant (ϵ') of pure

sample shows decrease in value with increase in frequency whereas dielectric constant (ϵ') of Dy doped CCTO samples show feeble frequency dependence especially in the range 1 kHz–1 MHz. For all doped and virgin samples, a sharp decrease of ϵ' is observed beyond 1 MHz. The drastic decrease in ϵ' at frequencies higher than 1 MHz may indicate the presence of conductive grains [4].

Sharp decrease in the dielectric constant in the MHz region shows the Debye like relaxation. High dielectric relaxation in CCTO may come from the Maxwell–Wagner effect at grain boundary [12]. The Maxwell–Wagner effect arises from the charge accumulation at interface of materials with different conductivities. It is believed that the double (back-to-back) Schottky potential barriers are created at the interfaces between n-type grains due to charge trapping at acceptor states, resulting in bending of the conduction band across the grain boundaries [13]. Acceptor concentration N_s at the grain boundaries increases due to Dy doping, in terms of the following Eq. (2). Then Schottky potential Φ_b may be enhanced resulting in a low dielectric constant by [14]

$$\phi_b = eN_s^2 / 8\epsilon_0\epsilon_r N_d \quad (2)$$

where e is the electronic charge, N_s is the acceptor (surface charge) concentration, vacuum permittivity $\epsilon_0 = 8.854 \times 10^{-12}$ F/m, ϵ_r is the relative permittivity of the material, and N_d is the charge carrier concentration in grains.

Dy addition greatly reduces the value of dielectric constant (ϵ'), which may be attributed to finer grain size. Effect of the Dy content on the frequency dependence of dielectric loss or $\tan(\delta)$ is shown in Fig. 3(b). Dielectric loss of pure CCTO is minimum with respect to doped samples in the frequency range from 100 Hz to 3 kHz but doped samples show lesser dielectric loss in the middle frequency range (~ 10 kHz to 1 MHz). Variation in the values of dielectric loss at lower frequencies may be attributed to electrode polarization.

Fig. 4(a) shows the variation of real part of dielectric constant (ϵ') of pure and Dy doped ceramics with temperature at different frequencies. Temperature dependence of dielectric constant of CCTO could be related to the excited deep trap states. At low temperature the interface is static because of the large relaxation time τ . This relaxation time decreases with increasing T and for $\omega\tau < 1$ the capacitance may be increased by the dynamic interface [13].

With increasing frequency, dielectric constant follows decreasing trend for all the samples. With increase in frequency, broad relaxation peak shifts towards higher temperature side. With increase in the Dy content, relaxation peaks are observed to shift towards low temperature side. All samples show negligible variation in dielectric constant with temperature at 1 kHz and 10 kHz in the temperature range 300–400 K which is a desired characteristics for devices.

Two relaxation processes are observed from the frequency and temperature dependence of dielectric constant. Low frequency relaxation is not observed clearly due to frequency range available for measurement at room temperature but as temperature increases dielectric constant shows increase while the broad relaxation peak shifts towards higher temperature

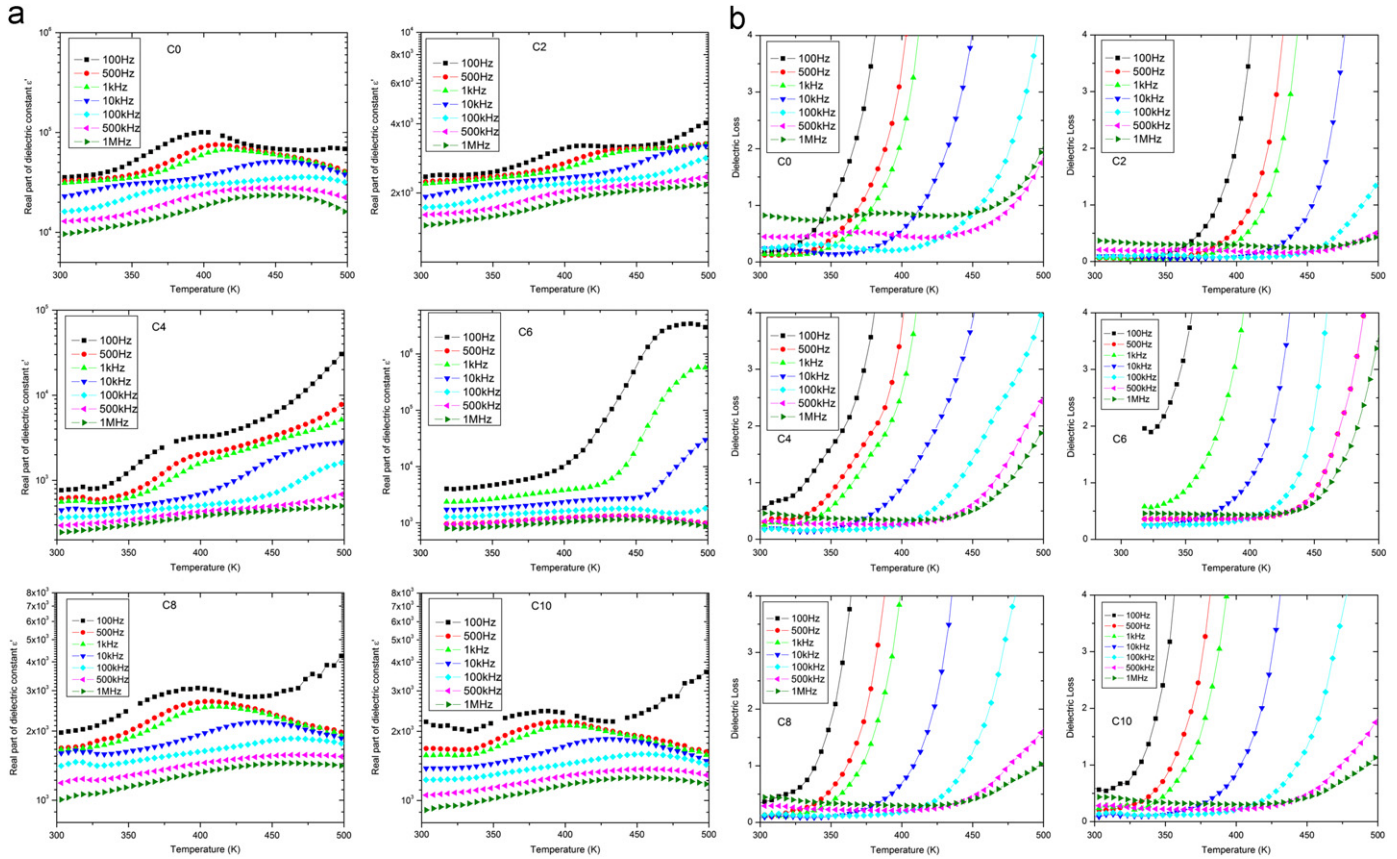


Fig. 4. (a) Variation of real part of dielectric constant ϵ' with temperature at different frequencies for pure and Dy doped samples. (b) Variation of dielectric loss with temperature at different frequencies for pure and Dy doped CCTO samples.

side with increase in frequency showing the Debye-like relaxation, low frequency relaxation is assumed to be associated with surface layers interfacial polarization [15].

Luo et al. [16] attributed low frequency relaxation to trap state related relaxation, which could be changed by electric conditioning but recover after releasing electric field. Therefore, maybe the large permittivity in the low frequency range of CCTO could be attributed to the trap states which exist in the electrode surface. Since the time is long enough to let the traps response, high permittivity is observed at low frequency. Doped samples show relaxation at lower frequencies at high temperature which may be attributed to hopping of trapped carriers.

Effect of Dy content on the temperature dependence of dielectric loss or $\tan(\delta)$ at different frequencies is shown in Fig. 4(b). Samples C2, C4, C8, and C10 show smaller loss than pure CCTO in the temperature range 300–350 K. It is observed that dielectric loss increases rapidly with increase in temperature. This rapid shoot-off in dielectric loss shifts towards higher temperature side with increasing frequency.

3.4. AC conductivity

Total conductivity (σ) in solids can be expressed as

$$\sigma = \sigma_{dc} + \sigma_{ac} \quad (3)$$

where, σ_{dc} is the DC conductivity which results from conduction band and σ_{ac} is the AC conductivity which originates from hopping conduction. σ_{ac} is an increasing function of frequency in disordered solids [17]. In the present study σ_{ac} was calculated using the relation

$$\sigma_{ac} = 2\pi f \epsilon_0 \epsilon' \tan(\delta) \quad (4)$$

where f is the frequency, ϵ_0 is the permittivity of vacuum, ϵ' is the real part of dielectric constant and $\tan(\delta)$ is the dielectric loss. Variation of σ_{ac} with frequency is shown in Fig. 5. Frequency dependence of σ_{ac} can be seen from AC power law [18]

$$\sigma_{ac} = A f^n \quad (5)$$

where A is the temperature dependent parameter, f is the frequency and frequency exponent n is dimensionless correlation coefficient having values between 0 and 1. In Fig. 5 (inset shows C8), frequency range can be divided into three regions namely regions I, II, III. In region I, since frequency is low, electric field does not influence the hopping conduction mechanism and conductance is almost equal to dc value. At low frequencies where the conductivity is constant, the transport takes place on infinite paths. In region II, conductivity starts increasing with frequency non-linearly. With further increase in frequency, conductivity increases linearly resulting in near constant

loss (NCL) [19]. At high frequency, conduction may be due to electron hopping between adjacent Ti-octahedron [17] and long range motion cannot occur. Increase in frequency increases hoping frequency and thereby increase in conductivity.

The exponent n can be calculated as a function of temperature by plotting $\ln \sigma_{ac}$ vs. $\ln f$ giving straight line with slope equal to exponent n . Values of exponent n for $x=0.0-0.1$ are in the range 0.58–0.78. CCTO is an interesting material with semiconducting grains and insulating grain boundaries [3]. Addition of Dy increases resistivity as can be seen from Figs. 5 and 6.

Variation of conductivity with frequency depends on number of potential barriers and their height. If a single charged species is to move in an infinite lattice of identical potential wells, the σ_{ac} is expected to be independent of frequency whereas in case of single particle hopping to and fro in a double well with infinite height, conductivity will increase and saturate at high frequency [20].

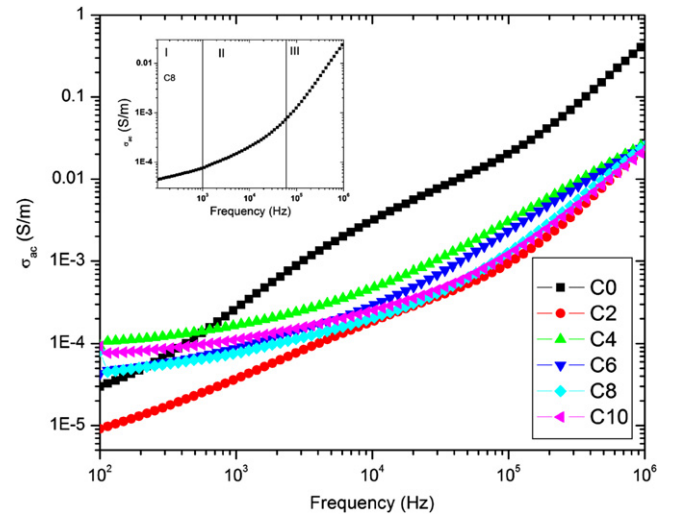


Fig. 5. Variation of AC conductivity σ_{ac} with frequency at different temperatures for pure and Dy doped CCTO samples.

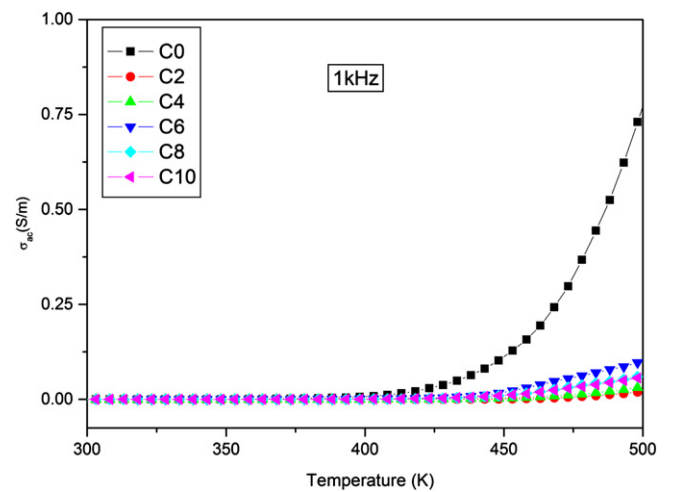


Fig. 6. Variation of AC conductivity σ_{ac} with temperature at 1 kHz for pure and Dy doped CCTO samples.

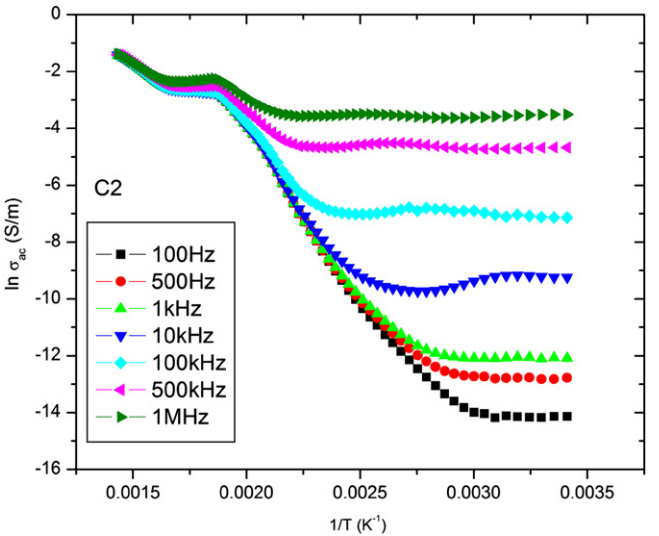


Fig. 7. Arrhenius plot between $1/T$ and $\ln \sigma_{ac}$ for Dy doped sample C2.

Table 2
Variation of activation energy obtained from AC process at low (300 K) and high (450 K) temperatures at 10 kHz.

Sample name	Activation energy (eV)	
	300 K	450 K
C0	0.733	0.023
C2	0.92	0.477
C4	0.729	0.336
C6	0.865	0.411
C8	0.835	0.413
C10	0.752	0.158

Arrhenius plot for sample C2 at different frequencies is shown Fig. 7. Plot between $1/T$ and $\ln (\sigma_{ac})$ gives the value of activation energy. According to Arrhenius principle,

$$\sigma_{ac} = \sigma_o \exp(-E_a/K_B T) \tag{6}$$

where σ_o is the pre-exponential factor, E_a is the Activation energy, T is the absolute temperature and K_B is the Boltzmann constant.

Values of activation energy for different Dy contents at 10 kHz and at low (280–333 K) and high (400–500 K) temperature regimes are given in Table 2. At high temperature side, activation energy is greatly reduced because thermal energy has greater role in affecting charge carriers' movement.

4. Conclusion

It is observed from XRD and Rietveld refinement that pure phase was retained after doping even after 10 mol% doping. It is observed that grain size is greatly affected by substitution of Dy in CCTO. With the substitution of Dy grain size decreases in all samples. It appears that higher doping concentrations, such as 8 and 10 mol%, result in coalescence in grains. Dielectric constant observed to be

decreased for Dy substitution. Sharp decrease in dielectric constant in the MHz region may be attributed to high frequency dielectric relaxation which comes from the Maxwell–Wagner effect arising from the charge accumulation at interface of materials with different conductivities. Doped samples show lower dielectric loss in the middle frequency range (from ~10 kHz to 1 MHz). Negligible variation in values of dielectric constant in 300–400 K at 1 kHz or 10 kHz, makes these materials suitable for device fabrication. At lower frequencies, σ_{ac} is close to dc conductivity and conduction is of long range behaviour while at high frequency, long range motion cannot occur. Activation energy is greatly reduced due to thermal energy gained by charge carriers at elevated temperature therefore an increase in conductivity is observed at high temperature.

Acknowledgement

Authors are thankful to the University of Delhi for providing financial support to carry out this work.

References

- [1] C.C. Homes, T. Vogt, S.M. Shapiro, S. Wakimoto, A.P. Ramirez, Optical response of high-dielectric-constant perovskite-related oxide, *Science* 293 (2001) 673–676.
- [2] M.A. Subramanian, D. Li, N. Duan, B.A. Reisner, A.W. Sleight, High dielectric constant in $\text{ACu}_3\text{Ti}_4\text{O}_{12}$ and $\text{ACu}_3\text{Ti}_3\text{FeO}_{12}$ phases, *Journal of Solid State Chemistry* 151 (2000) 323–325.
- [3] D.C. Sinclair, T.B. Adams, F.D. Morrison, A.R. West, $\text{CaCu}_3\text{Ti}_4\text{O}_{12}$: one-step internal barrier layer capacitor, *Applied Physics Letters* 80 (2002) 2153–2155.
- [4] T.B. Adams, D.C. Sinclair, A.R. West, Giant barrier layer capacitance effects in $\text{CaCu}_3\text{Ti}_4\text{O}_{12}$ ceramics, *Advanced Materials* 14 (2002) 1321–1323.
- [5] P. Lunkenheimer, R. Fichtl, S.G. Ebbinghaus, A. Loidl, Nonintrinsic origin of the colossal dielectric constants in $\text{CaCu}_3\text{Ti}_4\text{O}_{12}$, *Physical Review B* 70 (2004) 1–4 172102.
- [6] T.B. Adams, D.C. Sinclair, A.R. West, Influence of processing conditions on the electrical properties of $\text{CaCu}_3\text{Ti}_4\text{O}_{12}$ ceramics, *Journal of the American Ceramic Society* 89 (2006) 3129–3135.
- [7] R. Kashyap, O.P. Thakur, N.C. Mehra, R.P. Tandon, Effect of processing conditions on dielectric properties of $\text{CaCu}_3\text{Ti}_4\text{O}_{12}$ ceramics, *International Journal of Modern Physics B* 25 (2011) 1049–1059.
- [8] J. Li, M.A. Subramanian, H.D. Rosenfeld, C.Y. Jones, B.H. Toby, A.W. Sleight, Clues to the giant dielectric constant of $\text{CaCu}_3\text{Ti}_4\text{O}_{12}$ in the defect structure of $\text{SrCu}_3\text{Ti}_4\text{O}_{12}$, *Chemistry of Materials* 16 (2004) 5223–5225.
- [9] B.S. Prakash, K.B.R. Varma, Ferroelectriclike and pyroelectric behavior of $\text{CaCu}_3\text{Ti}_4\text{O}_{12}$ ceramics, *Applied Physics Letters* 90 (2007) 1–3 082903.
- [10] R. Kashyap, T. Dhawan, P. Gautam, O.P. Thakur, N.C. Mehra, R.P. Tandon, Effect of processing conditions on electrical properties of $\text{CaCu}_3\text{Ti}_4\text{O}_{12}$ ceramics, *Modern Physics Letters B* 24 (2010) 1267–1273.
- [11] L.E. Cross, Relaxor ferroelectrics, *Ferroelectrics* 76 (1987) 241.
- [12] B.S. Prakash, K.B.R. Varma, Effect of sintering conditions on the dielectric properties of $\text{CaCu}_3\text{Ti}_4\text{O}_{12}$ and $\text{La}_{2/3}\text{Cu}_3\text{Ti}_4\text{O}_{12}$ ceramics: a comparative study, *Physica B* 382 (2006) 312–319.
- [13] G. Blatter, F. Greuter, Carrier transport through grain boundaries in semiconductors, *Physical Review B* 33 (1986) 3952–3966.
- [14] T.B. Adams, D.C. Sinclair, A.R. West, Characterization of grain boundary impedances in fine- and coarse-grained $\text{CaCu}_3\text{Ti}_4\text{O}_{12}$ ceramics, *Physical Review B* 73 (2006) 1–9 094124.
- [15] L.F. Xu, P.B. Qi, X.P. Song, X.J. Luo, C.P. Yang, Dielectric relaxation behaviors of pure and Pr_6O_{11} -doped $\text{Cu}_3\text{Ti}_4\text{O}_{12}$ ceramics in high temperature range, *Journal of Alloys and Compounds* 509 (2011) 7697–7701.
- [16] X.-J. Luo, C.P. Yang, S.S. Chen, X.P. Song, H. Wang, K. Baerner, The trap state relaxation related polarization in $\text{Cu}_3\text{Ti}_4\text{O}_{12}$, *Journal of Applied Physics* 108 (2010) 1–5 014107.
- [17] A.M.M. Farea, S. Kumar, K.M. Batoo, A. Yousef, Alimuddin, Influence of frequency, temperature and composition on electrical properties of polycrystalline $\text{Co}_{0.5}\text{Cd}_x\text{Fe}_{2.5-x}\text{O}_4$ ferrites, *Physica B* 403 (2008) 684–701.
- [18] S.R. Elliott, A.c. conduction in amorphous chalcogenide and pnictide semiconductors, *Advances in Physics* 36 (1987) 135–217.
- [19] C. León, A. Rivera, A. Várez, J. Sanz, J. Santamaria, K.L. Nagi, Origin of constant loss in ionic conductors, *Physical Review Letters* 86 (2001) 1279–1282.
- [20] W. Li, R.W. Schwartz, Ac conductivity relaxation processes in $\text{CaCu}_3\text{Ti}_4\text{O}_{12}$ ceramics: grain boundary and domain boundary effects, *Applied Physics Letters* 89 (2006) 1–3 242906.